Nuclear translocation of the transcription factor STAT3 in the guinea pig brain during systemic or localized inflammation

Christoph Rummel, Thomas Hübschle, Rüdiger Gerstberger and Joachim Roth

Institut für Veterinär-Physiologie, Justus-Liebig-Universität Giessen, Frankfurter Strasse 100, D-35392 Giessen, Germany

The purpose of the present study was to investigate a possible lipopolysaccharide (LPS)-induced activation of brain cells that is mediated by the pleiotropic cytokine interleukin-6 (IL-6) and its transcription factor STAT3 during systemic or localized inflammation. In guinea pigs, intra-arterial (I.A., 10 μg kg^{-1}) or intraperitoneal (I.P., 30 μg kg^{-1}) injections of bacterial LPS cause a systemic inflammatory response which is accompanied by a robust fever. A febrile response can also be induced by administration of LPS into artificial subcutaneously implanted Teflon chambers (S.C. 100 or 10 μg kg^{-1}), which reflects an experimental model that mimics local tissue inflammation. Baseline plasma levels of bioactive IL-6 determined 60 min prior to injections of LPS or vehicle amounted to 35–80 international units (i.u.) ml^{-1}. Within 90 min of LPS injection, plasma IL-6 rose about 1000-fold in the groups injected I.A. or I.P., about 50-fold in the group injected S.C. with 100 μg kg^{-1} LPS, and only 5-fold in guinea pigs injected with the lower dose of LPS (10 μg kg^{-1}). At this time point, a distinct nuclear translocation pattern of the transcription factor STAT3 became evident in several brain structures. Amongst those, the sensory circumventricular organs known to lack a tight blood–brain barrier such as the area postrema, the vascular organ of the lamina terminalis and the subfornical organ, as well as the hypothalamic supraoptic nucleus showed intense nuclear STAT3 signals in the I.A. or I.P. injected groups. In contrast a moderate (S.C. group, 100 μg kg^{-1}), or even no (S.C. group, 10 μg kg^{-1}), nuclear STAT3 translocation occurred in response to S.C. injections of LPS. These results suggest that STAT3-mediated genomic activation of target gene transcription in brain cells occurred only in those cases in which sufficiently high concentrations of circulating IL-6 were formed during systemic (I.A. and I.P. groups) or localized (S.C. group, 100 μg kg^{-1}) inflammation.

Depending on the route of administration, bacterial lipopolysaccharide (LPS) induces a systemic or localized inflammatory response in experimental animal studies. Systemic inflammation is induced by intravenous, intra-arterial or intraperitoneal injection of LPS. Pro-inflammatory cytokines such as tumour necrosis factor (TNF)-α, interleukin (IL)-1β and IL-6 are regarded as key mediators for the manifestation of fever under these experimental conditions (for review, see Kluger, 1991; Dinarello, 1999). In response to LPS administration via the systemic routes mentioned above, these cytokines and LPS itself are measurable in the circulation at increased concentrations (Givalois *et al.* 1994; Lenczowski *et al.* 1997; Roth *et al.* 1998; Romanovsky *et al.* 2000; Johnson

et al. 2003). Alternatively, experimental models have been established in which LPS is administered locally, rather than systemically, into a subcutaneous air pouch in rats (Miller *et al.* 1997*a*; Cartmell *et al.* 1999), or into a subcutaneously implanted artificial Teflon chamber in guinea pigs (Ross *et al.* 2000). These models nicely mimic localized tissue inflammation that is usually accompanied by a febrile response. Interestingly, LPS, TNF-α and IL-1β rarely enter the circulation from the site of localized subcutaneous inflammation, while IL-6 is consistently increased in plasma (Miller *et al.* 1997*b*; Cartmell *et al.* 2000, 2001; Ross *et al.* 2000, 2003; Turnbull *et al.* 2003). IL-6 might therefore be the only cytokine implicated in LPS-induced fever that can be measured in significant quantities

in the circulation during both systemic and localized inflammatory responses, while other pyrogenic cytokines such as TNF-α and IL-1β are measurable only when LPS is administered via systemic routes. Consequently, circulating IL-6 has been hypothesized as an important afferent signal to be integrated at the level of the central nervous system and to contribute to classical signs of illness such as fever, sickness behaviour or the activation of the hypothalamo-pituitary-adrenal (HPA) axis (Cartmell *et al.* 2000; Dantzer, 2001; Turnbull *et al.* 2003). Further evidence for such a role of IL-6 is based on the following sets of observations. (i) There is an excellent correlation between the plasma concentration of IL-6 and the strength of fever in human patients (Nijsten *et al.* 1987) and experimental animals (LeMay *et al.* 1990; Roth *et al.* 1993, 1994). (ii) The febrile response to LPS is abrogated and the activation of the HPA axis during localized inflammation is blunted in IL-6-deficient ('knockout') mice (Chai *et al.* 1996; Turnbull *et al.* 2003). (iii) Systemic administration of antibodies against rat IL-6 depresses fever in rats which develops after injection of LPS into a subcutaneous air pouch (Cartmell *et al.* 2000). The authors of the latter study suggested that the elevated concentrations of circulating IL-6 during localized inflammation, albeit being moderate, might gain entry into the brain via an active transport system (Banks *et al.* 1994) or via sites of the brain lacking a tight blood–brain barrier such as the circumventricular organs (CVOs) (Blatteis *et al.* 1983, 1987; Blatteis & Sehic, 1997). With elevated circulating concentrations of IL-6 active as humoral signals on the brain at the level of the CVOs, it should be possible to demonstrate a direct action of this cytokine on cellular elements within these specialized brain structures during systemic or localized inflammation.

IL-6-induced signal transduction starts with the binding of IL-6 to a specific receptor subunit. Then a second signal transducing subunit named gp130 associates with the ligand–receptor complex. Together, these three molecules induce signal transduction in target cells for IL-6 (Taga & Kishimoto, 1997; Heinrich *et al.* 1998). Homodimerization of gp130 to the complex of IL-6 and its receptor activates a specific signal transduction pathway, the so-called Janus kinase – signal transducer and activator of transcription (JAK-STAT) signalling cascade. The first step within this cascade is the activation of gp130-associated cytoplasmatic tyrosine kinases (JAKs). Then, the STAT3 isoform of this group of transcription factors is phosphorylated, dimerizes and translocates into the nucleus of the IL-6-stimulated cell, where it regulates gene expression by binding to specific gene promoters (Takeda & Akira, 2000). An accumulation of STAT3 in the nuclei of brain cells can

be visualized by immunohistochemistry in rats treated with LPS or IL-6 (Konsman *et al.* 2000; Hübschle *et al.* 2001; Gautron *et al.* 2002; Harré *et al.* 2002). Due to the fact that peripheral injections of LPS or IL-6 activate the same brain zones, LPS-induced nuclear STAT3 activation mediated by IL-6 was postulated (Harré *et al.* 2002, 2003). Thus, STAT3 immunohistochemistry proved to be an excellent tool to demonstrate IL-6-induced genomic activation of brain cells during fever and this was clearly shown by our group in the rat (Hübschle *et al.* 2001; Harré *et al.* 2002).

In the present study we evaluated this approach in guinea pigs under conditions of localized *versus* systemic inflammatory responses. We therefore administered LPS via systemic (intra-arterial, I.A.; intraperitoneal, I.P.) and local (subcutaneous chamber, S.C.) routes in guinea pigs. Fever and circulating concentrations of IL-6 were measured and related to nuclear translocation of STAT3 in brain areas implicated in fever, namely the so-called sensory CVOs: the vascular organ of the lamina terminalis (OVLT), the subfornical organ (SFO) and the area postrema (AP). Due to their dense vascularization with a fenestrated endothelium surrounded by perivascular spaces these brain structures have been discussed as sensors for chemical messengers, which are transported by the bloodstream, including pyrogenic cytokines such as IL-6. Special attention was directed to the question of whether the comparably moderate increase in circulating IL-6 during a localized inflammatory response is sufficient to induce a direct activation of cellular elements within the brain.

Methods

Animals

Male guinea pigs (*Cavia aperea porcellus*) with a body weight of 380–400 g on the day of surgery were used in all experiments. The animals were housed in individual cages in a controlled environment at an ambient temperature of $22°C$ on a 12 h : 12 h light–dark cycle (light off at 19.00 h). The animals had access to food and water *ad libitum*. Twice a week the reservoirs were filled with fresh hay, pellet food and water and at the same time the cages were changed. About 10 days before the experiment, the animals were prepared surgically (see below) and habituated at least twice to the experimental handling procedures. The national guidelines for experiments with vertebrate animals were followed and local ethics committee approval was obtained from the regional government for the experimental protocols (reference number GI 18/2-42/00).

Surgery

Guinea pigs were chronically implanted with intra-arterial catheters for blood sampling and injections as well as intra-abdominal radiotransmitters for the measurement of body core temperature. Some groups of animals were additionally implanted with artificial subcutaneous Teflon (polytetrafluoroethene) chambers equipped with catheters for injections. Briefly, the guinea pigs were anaesthetized with $100 \, mg \, kg^{-1}$ ketamine hydrochloride (Pharmacia Upjohn, Erlangen, Germany) and $0.25 \, mg \, kg^{-1}$ medetomidine hydrochloride (Pfitzer GmbH, Karlsruhe, Germany). A polyethylene catheter (Portex, Kent, UK; 0.4 mm inner diameter, 0.8 mm outer diameter) was inserted through the left carotid artery until it reached the aortic arch. Slow aspiration of blood with a syringe indicated the correct position of the catheters. The catheter was then fixed with two sutures. The distal end of the catheter was tunnelled subcutaneously to the interscapular region of the back where it was exteriorized and again fixed with two sutures. The muscle layer and the skin were closed separately with sutures. Finally, the catheter was flushed with sterile heparinized saline and sealed by heating.

The Teflon chambers were implanted into subcutaneous cavities which were formed with a cylindrical Plexiglas stick after a cutaneous incision. The cavities which existed after removing the Plexiglas stick had about the same diameter and size as the artificial subcutaneous chamber which was open at both ends. The open sides of the cylindrical chambers with an inner diameter of 10 mm had close contact to the skin tissue. The subcutaneous chamber was placed laterally to the dorsal midline, caudally to the scapulae of the anaesthetized guinea pigs. The chambers were equipped with catheters for administration of drugs, which were also tunnelled subcutaneously to the interscapular region of the back, caudally to the arterial catheter and sealed by heating. Then the skin was closed with sutures (for details about size and shape of the sub-cutaneous chambers see Ross *et al.* 2000, 2003). After surgical placement of arterial catheter and subcutaneous chamber, a biotelemetry transmitter for measurement of core temperature was implanted intraperitoneally.

LPS

Bacterial LPS (derived from *Escherichia coli*, Sigma Chemicals, St Louis, MO, USA) was suspended in sterile pyrogen-free 0.9% saline at different concentrations. LPS was administered I.A. at a dose of $10 \, \mu g \, kg^{-1}$ (prepared from a $10 \, \mu g \, ml^{-1}$ solution), I.P. at a dose of $30 \, \mu g \, kg^{-1}$ (prepared from a $30 \, \mu g \, ml^{-1}$ solution), or s.c. into the implanted Teflon chambers at a high dose of $100 \, \mu g \, kg^{-1}$ (prepared from a $100 \, \mu g \, ml^{-1}$ solution) or a low dose of $10 \, \mu g \, kg^{-1}$ (prepared from a $10 \, \mu g \, ml^{-1}$ solution). Equivalent volumes of the vehicle were injected in control groups. The LPS doses were chosen according to previous studies from our laboratory (Goldbach *et al.* 1997; Roth *et al.* 1998; Ross *et al.* 2000, 2003).

Collection of plasma

During the experiments, blood samples (about 0.6 ml per sample) were slowly drawn from the intra-arterial catheter into sterile heparinized syringes and immediately centrifuged. After each blood sampling procedure, the catheter was flushed with a small volume (about 0.1 ml) of heparinized saline (about 80 i.u. of heparin) and closed by heating. After centrifugation of the sample, plasma was stored at $-70^\circ C$ for later determination of bioactive IL-6. In the 2–3 days before an experiment, the animals were accustomed to the blood sampling procedure at least twice, which then did not cause excitement or stress-induced changes of body temperature.

Experimental protocol

Experiment 1. Seven groups of guinea pigs ($n = 5$–6 per group) were injected I.A. with either $10 \, \mu g \, kg^{-1}$ LPS or an equivalent volume of the vehicle (0.9% NaCl), or I.P. with either $30 \, \mu g \, kg^{-1}$ LPS or vehicle, or s.c. with $100 \, \mu g \, kg^{-1}$ LPS, $10 \, \mu g \, kg^{-1}$ LPS or vehicle. Body core temperature was evaluated from 2 h before, until 6 h after, the respective injection. Blood samples were taken via the intra-arterial catheters 1 h before, and 90 min after, injection for later determination of bioactive IL-6. The first sample was used to determine the basal concentration of bioactive IL-6 in each investigated animal. The second time point was chosen, because IL-6-mediated activation of brain cells via the transcription factor STAT3 was quantitatively analysed 90 min after stimulation with LPS or vehicle (see below).

Experiment 2. Another seven groups of guinea pigs ($n = 3$–4 per group) were injected with LPS or vehicle according to the schedule of experiment 1. The brains of all animals were prepared for STAT3 immuno-histochemistry 90 min after injection. Guinea pigs were deeply anaesthetized with sodium pentobarbital (60–$100 \, mg \, kg^{-1}$, Narcoren, Merial GmbH, Hallbergmoos, Germany) and transcardially perfused with 400 ml 0.9% NaCl solution followed by 500 ml of fixative containing 4% paraformaldehyde in 0.1 M phosphate buffer (pH 7.2). The

brains were removed and postfixed in the same fixative for 1 h at room temperature. The tissue was cryoprotected in 20% sucrose in phosphate buffer overnight at 4°C. Brain tissue was cut the following day.

Measurement of body temperature

Abdominal temperature was measured by use of intra-peritoneally implanted (see above) battery-operated biotelemetry transmitters (PDT-4000 E-mitter; Mini-Mitter Co., Sunriver, OR, USA). Output (frequency in Hz) was monitored by an antenna placed under each cage (ER-4000 radioreceivers, Mini-Mitter). A data acquisition system (VitalView, Mini-Mitter) was used for automatic control of data collection and analysis. Body temperature was monitored and recorded at 5 min intervals. For the analysis and graphical documentation, temperature data at time intervals of 15 min were used.

IL-6 bioassay

Determination of IL-6 was performed by a bioassay based on the dose-dependent growth stimulation of IL-6 on the mouse B9 hybridoma cell line (Aarden *et al.* 1987). The assay was performed in sterile, 96-well microtitre plates. In each well, 5000 B9 cells were incubated for 72 h with serial dilutions of biological samples or with different concentrations of a human IL-6 standard (code 89/548, National Institute for Biological Standards and Control, South Mimms, UK). Plasma samples were pre-diluted so that serial dilution of samples and standard dilution curves were parallel. The number of living cells after 72 h was measured by use of the dimethylthiazol-diphenyl tetrazolium bromide (MTT) colorimetric assay (Holt *et al.* 1991). The detection limit of the assay, after considering the dilution of samples into the assays, was 3 i.u. IL-6 ml^{-1}.

STAT3 immunohistochemistry

To detect STAT3 signals in the guinea pig brain, free-floating sections were incubated with a rabbit anti-STAT3 antibody (sc-482, Santa Cruz Biotechnology, Heidelberg, Germany). Previous studies investigating STAT3 distribution in the rat central nervous system have shown that amplification procedures are a helpful tool for investigating STAT3 immunoreactivity (Strömberg *et al.* 2000; Hübschle *et al.* 2001). Therefore, a commercial tyramide amplification kit (NEL700, NEN Life Science Products, Cologne, Germany), based on the catalysed reporter deposition amplification method, was used. Controls for STAT3 immunoreactivity included processing

sections without the primary antibody, or incubating sections with rabbit preimmune serum instead of rabbit anti-STAT3 antiserum. In both cases no STAT3 immuno-reactivity was found in any brain area. Finally, the specificity of the STAT3 immunohistochemistry was proven by preadsorbing the primary antibodies with the antigen. The results of these preadsorption experiments are available online as Supplementary Material to this article, because the specificity of STAT3 immunohistochemistry has not yet been documented in guinea pigs. Incubation of the STAT3 antibody with an amount of antigen which corresponded to a 75-fold molecular weight excess resulted in an almost complete abrogation of STAT3 immuno-reactivity on the brain sections. Virtually no nuclear STAT3 signals were observed in this case.

Coronal 40 μm brain sections were cut on a freezing microtome (model 1205, Jung, Heidelberg, Germany). Tyramide amplification staining was performed according to the kit description, but in a phosphate buffer system (pH 7.2); the details are as follows. Sections were placed into 10% normal horse serum containing 0.3% Triton X-100 for 1 h at room temperature. They were then transferred into 0.5% blocking powder to block the unspecific tyramine binding sites. Primary STAT3 anti-body incubation (dilution 1 : 12 000) was performed for 36–48 h at 4°C. The STAT3 antibody was then detected with a secondary biotinylated antirabbit antibody (1 : 200, vector BA-1000, Linaris Biologische Produkte, Wertheim-Bettingen, Germany) for 1 h at room temperature. After amplification, the immunohistochemical processing was finished with an avidin biotin horseradish peroxidase complex (Vector Elite Kit, Linaris Biologische Produkte), which was visualized by a diaminobenzidine hydro-chloride (Sigma Chemicals) reaction in the presence of hydrogen peroxide. Finally, sections were counter-stained with cresyl violet and coverslips applied with Entellan (Merck, Darmstadt, Germany) for light micro-scope analysis.

Sections were analysed using an Olympus BX50 light microscope (Olympus Optical, Hamburg, Germany). Digital images were taken with an Olympus Camedia C-3030 camera and the Olympus Camedia Master 2.0 software package. Image editing software (Adobe Photo-shop) was used to adjust brightness and contrast, to change the graphic mode to CMYK, and to combine the individual images into the figure plates.

The numbers of STAT3-immunoreactive cell nuclei were quantitatively evaluated for the three sensory CVOs: the AP (Fig. 3), the OVLT (Fig. 4) and the SFO (Fig. 5), and for the hypothalamic supraoptic nucleus (SON, Fig. 6), 90 min after systemic or local treatment with LPS or sterile saline.

This time point was chosen according to pilot experiments, in which we observed an LPS-induced nuclear STAT3 translocation in brain cells of guinea pigs starting 60 min after LPS administration and reaching maximal values 90–120 min after treatment with LPS. For each animal, three caudal to medial AP sections, three rostral OVLT sections, three medial SFO sections, and three sections from the rostral SON level were selected. A microscopic counting grid (200 μm $\times$ 200 μm) was used at $\times$400 magnification to determine number of STAT3-positive cell nuclei per section within the AP, the OVLT, the SFO and the SON of each investigated animal. The quantitative data shown in Fig. 7 therefore finally represent the means (three sections from each structure per individual animal) of the means (animals of a given group).

Evaluation and statistics

Thermal responses to injections of LPS or vehicle abdominal temperatures of the different experimental groups were plotted against time and expressed as means $\pm$ s.e.m. at each time point. Abdominal temperatures of LPS-treated *versus* vehicle-treated guinea pigs were compared by two-way repeated measures ANOVA followed by an all pairwise Bonferroni's multiple comparison *post hoc* test (Sigmaplot/Sigmastat analysis software, Jandel Scientific, SPSS Science Software GmbH, Erkrath, Germany). The fever index as the integrated area under the fever curve was further used to compare the strength of the febrile responses. The mean of all temperatures measured at 15 min intervals over the 2 h before injection of LPS or saline was used as the baseline temperature for the calculation of each individual fever index. Fever indices between the experimental groups were compared by one-way ANOVA followed by Scheffe's *post hoc* test (StatView, Abacus Concepts, Berkeley, CA, USA). Circulating levels of IL-6 and numbers of STAT3-immunoreactive cell nuclei in specific brain areas were also compared between the experimental groups by one-way ANOVA and Scheffe's test. Because the values for cytokine concentrations and numbers of STAT3-positive cell nuclei were not normally distributed, a log-transformation was performed before the statistical calculations.

Results

Fever and circulating IL-6 in response to systemic or local administration of LPS

I.A. (10 μg kg^{-1}), I.P. (30 μg kg^{-1}) or S.C. (100 or 10 μg kg^{-1}) injections of LPS evoked fever in guinea pigs when

compared to the respective control groups which were treated with sterile saline (upper and middle panels of Fig. 1). Calculation of the fever indices (the areas under the fever curves, lower panel of Fig. 1) revealed that the overall strength and duration of LPS-induced fever was similar in the I.A. and I.P. injected groups and in guinea pigs in which
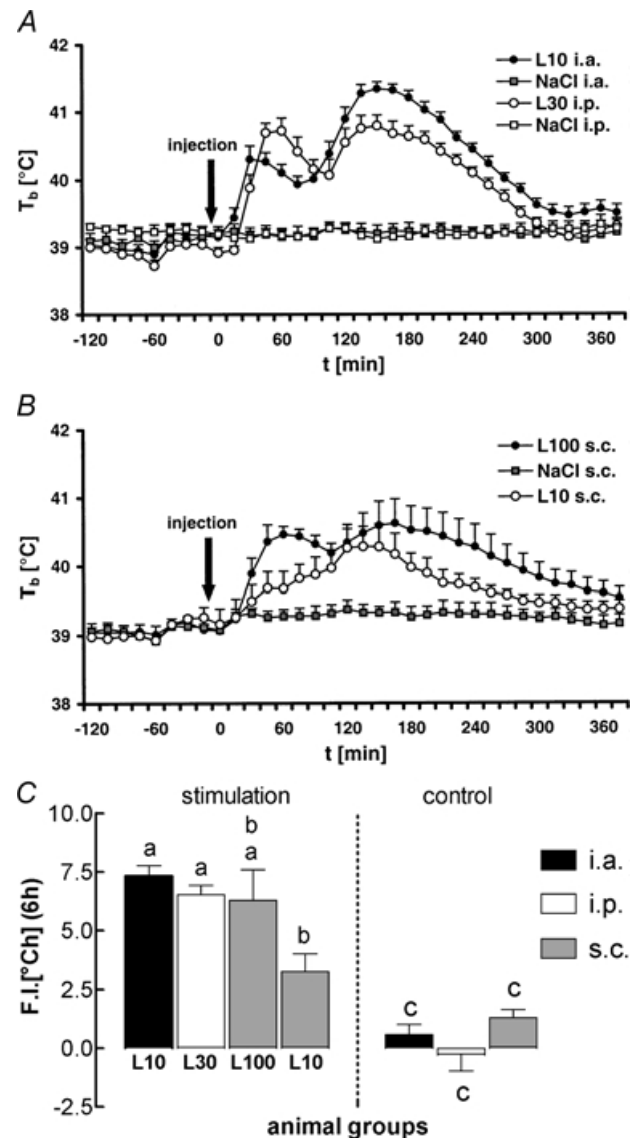

Figure 1. Febrile responses of guinea pigs injected I.A., I.P. or S.C. with lipopolysaccharide (LPS) or vehicle

A, febrile responses (T_b, body temperature) of guinea pigs injected I.A. (10 μg kg^{-1}, black circles, $n = 6$) or I.P. (30 μg kg^{-1}, open circles, $n = 6$) with LPS or vehicle (NaCl I.A., grey squares, $n = 5$; NaCl I.P. open squares, $n = 5$). *B*, febrile responses of guinea pigs injected S.C. with LPS (100 μg kg^{-1}, black circles, $n = 6$; 10 μg kg^{-1}, open circles, $n = 6$) or vehicle (NaCl S.C., grey squares, $n = 5$). *C*, integrated areas under the curves (fever index; F.I.) shown in *A* and *B*. Any columns with the same letter are not significantly different from each other, while any columns with different letters are significantly different ($P < 0.05$). All symbols and columns are means $\pm$ s.e.m.

the higher dose of LPS was administered into the subcutaneous chamber. The integrated fever response to s.c. injections of the lower LPS dose was significantly smaller when compared to the responses of guinea pigs injected i.a. or i.p. with LPS, but not when compared to fever in animals treated s.c. with $100 \mu g \, kg^{-1}$ LPS. However, from 45 to 105 min after s.c. injections of LPS, the high dose evoked a significantly stronger increase in the animals' body core temperature in comparison to the low dose (two-way repeated measures ANOVA with Bonferroni's *post hoc* test).

One hour prior to the injections of LPS or vehicle, mean levels of IL-6 in plasma were in the range of 35–80 i.u. ml^{-1} in all of the seven investigated groups. When compared to these preinjection values, IL-6 in plasma significantly rose within 90 min of administration of the pyrogen in all four LPS-treated groups ($P < 0.0001$ for the groups injected i.a. with $10 \mu g \, kg^{-1}$, i.p. with $30 \mu g \, kg^{-1}$, or s.c. with $100 \mu g \, kg^{-1}$; $P = 0.0069$ for the group injected s.c. with $10 \mu g \, kg^{-1}$; ANOVA). In the groups injected i.a., i.p. or s.c. with vehicle, circulating levels of IL-6 in plasma 90 min after injection were not significantly different from the preinjection values. The levels of IL-6 in plasma from all seven experimental groups, measured 90 min after injection of LPS or vehicle, are summarized in Fig. 2.

In guinea pigs treated i.a. or i.p. with LPS we observed a dramatic increase of circulating IL-6 to mean values of 57 727 i.u. ml^{-1} (i.a. group), or 30 616 i.u. ml^{-1} (i.p. group). Injection of LPS s.c. resulted in a far less pronounced rise of IL-6 in plasma, to 2527 i.u. ml^{-1}

($100 \mu g \, kg^{-1}$), or 591 i.u. ml^{-1} ($10 \mu g \, kg^{-1}$). The values measured in all of the four LPS-treated groups were significantly different from each other. Compared to the groups treated i.a. or i.p. with sterile saline, guinea pigs injected s.c. with the vehicle, showed a slightly but significantly elevated level of circulating IL-6 (114 i.u. ml^{-1}; $P = 0.0288$, saline s.c. *versus* saline i.a.; $P = 0.0278$, saline s.c. *versus* saline i.p.). This observation was interpreted as a sign of a moderate inflammatory response caused by the implanted subcutaneous chamber in addition to the intra-arterial catheter.

In summary, administration of LPS in guinea pigs caused fever irrespective of the route of injection. The febrile response was accompanied by a drastic rise in circulating IL-6 when LPS was administered via systemic routes, and a moderate increase of IL-6 in plasma when LPS was injected locally into a subcutaneous chamber.

Nuclear STAT3 translocation in brain cells in response to systemic or local administration of LPS

To test the hypothesis that the circulating amount of bioactive IL-6, which is measurable in response to i.a., i.p. or s.c. administrations of LPS, may be sufficient to act as a humoral signal to the brain, STAT3 immunohistochemistry was performed with brain sections prepared 90 min after systemic or local injections of LPS or vehicle in guinea pigs. We observed translocation of the transcription factor STAT3 into the nucleus of cells in several brain areas (Table 1).

In a few brain structures such as the hippocampus, the hypothalamic periventricular nucleus and the ventro-medial preoptic nucleus, nuclear STAT3 translocation was exclusively observed when LPS was administered via systemic routes (i.a. or i.p.). In some other structures such as the arcuate nucleus, the median eminence, the meninges, or endothelial cells, a few nuclear STAT3 signals were observed even under control conditions (i.a., i.p. or s.c. injections of sterile saline). In these structures STAT3 activation seemed to be up-regulated by systemic and, in part, by local treatment with LPS. The sensory CVOs (AP, OVLT, SFO) and the hypothalamic SON belonged to those brain areas in which LPS caused the most pronounced nuclear translocation of STAT3 when compared to the respective controls. Therefore nuclear STAT3 translocation in these brain structures were documented qualitatively (Figs 3–6, Table 1) and quantitatively (Fig. 7).

The microphotographic illustrustrations in Figs 3–6 are all shown in a similar way. An overview of a particular brain region with the respective sensory CVO or with
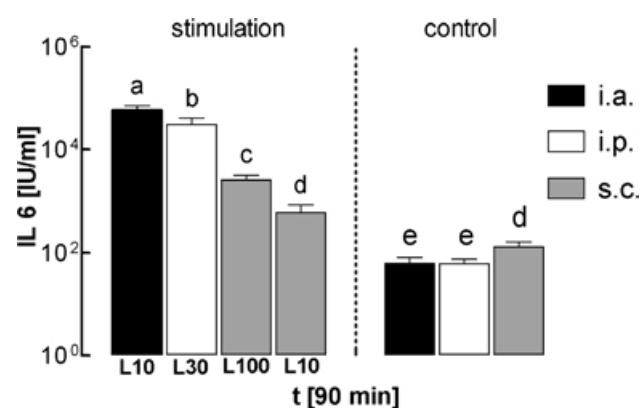
Figure 2. Circulating IL-6 in guinea pigs injected I.A., I.P. or S.C. with LPS or vehicle
Circulating levels of bioactive IL-6 measured 90 min after injection of LPS or vehicle (0.9% NaCl) via different routes (I.A., black columns; I.P., open columns; S.C., grey columns). The groups correspond to those shown in Fig. 1. Any columns with the same letter are not significantly different from each other, while any columns with different letters are significantly different ($P < 0.05$). All columns are means ± S.E.M.

Table 1. Distribution of nuclear STAT3 expression in the guinea pig brain

Brain structures	LPS 10 μg kg^{-1} I.A.	LPS 30 μg kg^{-1} I.P.	LPS 100 μg kg^{-1} S.C.	LPS 10 μg kg^{-1} S.C.	NaCl I.A.	NaCl I.P.	NaCl S.C.
Forebrain							
Hippocampus (CA1–CA3)	+ +	+	−	−	−	−	−
Caudate putamen	+	−	−	−	−	−	−
Hypothalamus and preoptic area							
Supraoptic nucleus	+ + +	+ +	+	−	−	−	−
Paraventricular nucleus	−	−	−	−	−	−	−
Periventricular nucleus	+ + +	+	−	−	−	−	−
Ventromedial preoptic nucleus	+ +	+	−	−	−	−	−
Arcuate nucleus	+ +	+ +	+ +	+	+	+	+
Circumventricular organs							
Vascular organ of the lamina terminalis	+ + +	+ + +	+	− +	−	−	−
Subfornical organ	+ +	+ +	+	−	−	−	−
Area postrema	+ + +	+ + +	+ +	− +	−	−	−
Median eminence	+ +	+ +	+ +	+	+	+	+
Brainstem							
Nucleus of the solitary tract	+	− +	−	−	−	−	−
Others							
Meninges	+ + +	+ + +	+ +	+	+	+	+
Endothelial cells	+ +	+ +	+	+	− +	− +	− +
Ependymal lining of all ventricles	+ + +	+ +	+	− +	− +	− +	− +
Choroid plexus	+ +	+	+	− +	− +	− +	− +

Distribution of nuclear STAT3 signals in the guinea pig brain during control (NaCl-treated groups) and LPS-stimulated conditions. Relative values of nuclear STAT3 immunoreactivity are given as estimates of the density of nuclear STAT3 labelling in the seven experimental animal groups. STAT3 signals were analysed 90 min after systemic (10 μg kg^{-1} LPS I.A., 30 μg kg^{-1} LPS I.P.) or local subcutaneous (100 μg kg^{-1} LPS S.C., 10 μg kg^{-1} LPS S.C.) injection of LPS or equivalent volumes of vehicle (NaCl I.A., I.P. or S.C.). A five point scale was used to rate the data: + + + = high density of nuclear STAT3 signals, + + = medium to moderate density, + = low density, − + = single nuclear signals in some cases, − = no nuclear signals. The guinea pig brain nomenclature given here has been adapted and slightly modified from that used by Paxinos & Watson (1998) for the rat brain.

the SON is shown in panel *A* (AP in Fig. 3*A*, OVLT in Fig. 4*A*, SFO in Fig. 5*A*, SON in Fig. 6*A*). Panel *B* shows the brain region under one of the three control conditions (Fig. 3*B*: AP after s.c. injection of vehicle; Fig. 4*B*: OVLT after I.A. injection of vehicle; Fig. 5*B*: SFO after I.P. injection of vehicle; Fig. 6*B*: SON after I.P. injection of vehicle). Irrespective of the route of administration, treatment with sterile saline did not induce nuclear STAT3 translocation in any of these brain structures. Panels *C* and *D* in Figs 3–6 demonstrate pronounced numbers of STAT3-positive cell nuclei in sensory CVOs and in the hypothalamic SON of guinea pigs treated I.A. or I.P. with LPS. Depending on the individual CVO a high to moderate (AP) or low (OVLT, SFO) density of nuclear STAT3 signals was observed in response to s.c. injections of 100 μg kg^{-1} LPS (panel *E* in Figs 3–6). Just a few, or even no (SFO), nuclear STAT3 signals were observed in response to s.c. administration of 10 μg kg^{-1} LPS. In the hypothalamic SON a similar pattern of the strength of nuclear STAT3 signals was determined (panel *F* in Figs 3–6).

From all investigated CVOs the AP showed the highest number of STAT3-positive cell nuclei (Fig. 3). In controls as well as in LPS-treated guinea pigs strong STAT3 immunoreactivity was detected at the border of the AP towards the 4th ventricle. This labelling most likely included cells of the so-called glia limitans. However, few nuclear STAT3 signals were detected in control groups in this structure when compared to LPS-treated animals. A further brain region in close vicinity to the AP that showed strong STAT3 immunoreactivity at this brain level proved to be the dorsal vagal motor complex, including the nucleus of the solitary tract (NTS) and the dorsal motor nucleus of the vagus. However, with the exception of a few nuclear signals in guinea pigs treated I.A. with LPS, the observed immunoreactivity in this brain area was of cytoplasmic origin. As for the nuclear signals within the AP, a spatial pattern of STAT3 immunoreactivity was observed. In the rostral part of the AP, nuclear signals occurred throughout the entire area of this CVO (not shown). In animals treated with LPS I.A. or I.P., nuclear signals in medial to caudal aspects of the AP were often clustered in a V-shaped arrangement towards the border to the NTS (Fig. 3*C*).

With respect to the strength of nuclear STAT3 immunoreactivity, the second largest number of signals was
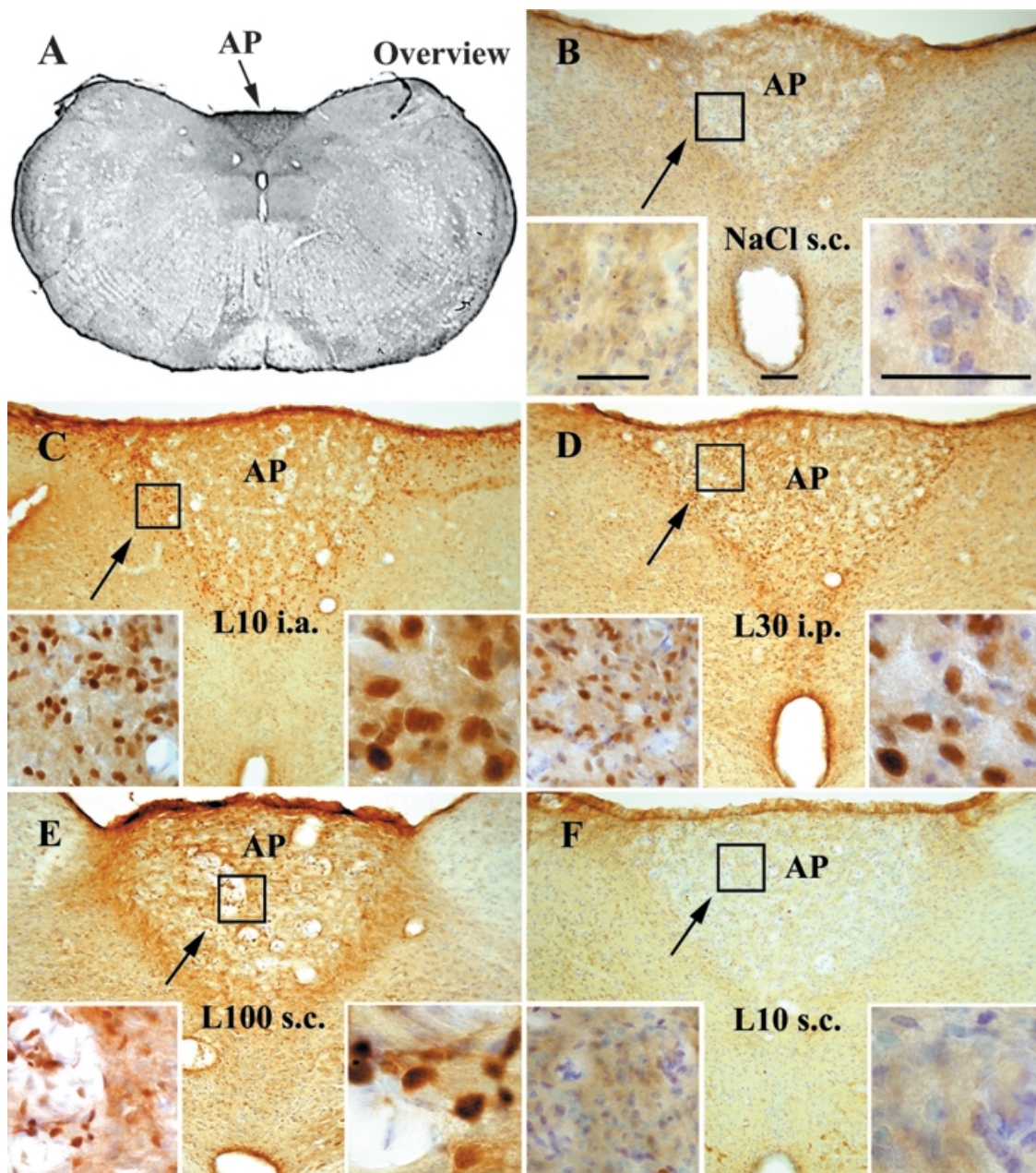
Figure 3. STAT3 immunoreactivity in the area postrema (AP) of guinea pigs injected systemically or locally with LPS or vehicle

Representative photomicrographs of the medial to caudal AP (arrows) are shown in an overview (A) during non-stimulated (B) and LPS-stimulated (C–F) conditions. STAT3 immunoreactivity was observed in seven groups of guinea pigs 90 min after injections with LPS (10 μg kg^{-1} I.A. (L10 i.a.) $n = 4$; 30 μg kg^{-1} I.P. (L30 i.p.) $n = 3$; 100 μg kg^{-1} S.C. (L100 s.c.) $n = 4$; or 10 μg kg^{-1} S.C. (L10 s.c.) $n = 4$) or with an equivalent volume of vehicle (NaCl I.A., $n = 3$; NaCl I.P., $n = 3$; or NaCl S.C., $n = 3$). Note that the specific STAT3 immunoreactivity is shown by the brown reaction product as a result of diaminobenzidine hydrochloride conversion. Cresyl violet counterstaining was used to label cell nuclei and depict general neuroanatomy. Specific nuclear STAT3 labelling induced by systemic (C and D) or local LPS treatment (E and F) is shown at higher magnifications in the insets and compared with the blue-coloured cell nuclei from the control situation (B). Bar in B represents 100 μm. Bars on the right insets represent 50 μm.

observed in the OVLT (Fig. 4). Intense nuclear STAT3 labelling was found in rostral and medial areas of this CVO. In the subdistribution of these signals, a high density was observed in dorsolateral parts of the OVLT extending to the adjacent ventromedial preoptic area. (Fig. 4*C* and *D*). In animals treated s.c. with LPS, nuclear STAT3 signals rarely occurred and were predominantly observed in the lateral parts of the OVLT (Fig. 4*E*). Similar to the observation made in the AP, meningeal cells showed high STAT3 immunoreactivity, however, with a pronounced number of nuclear signals only in guinea pigs treated systemically (i.a. or i.p.) with LPS.

From all of the three sensory CVOs the lowest density of nuclear STAT3 signals in LPS-treated guinea pigs was observed in the SFO (Fig. 5). While systemic LPS treatment resulted in nuclear STAT3 translocation throughout the entire SFO (Fig. 5*C* and *D*), s.c. injections of 100 μg kg^{-1} LPS tended to cause activation of just the lateral parts of this CVO (Fig. 5*E*). In response to s.c. administration of the low LPS dose, virtually no nuclear STAT3 signals in the SFO were detected at all.

Surprisingly, treatment with LPS resulted in nuclear translocation of STAT3 in brain areas reported to possess a
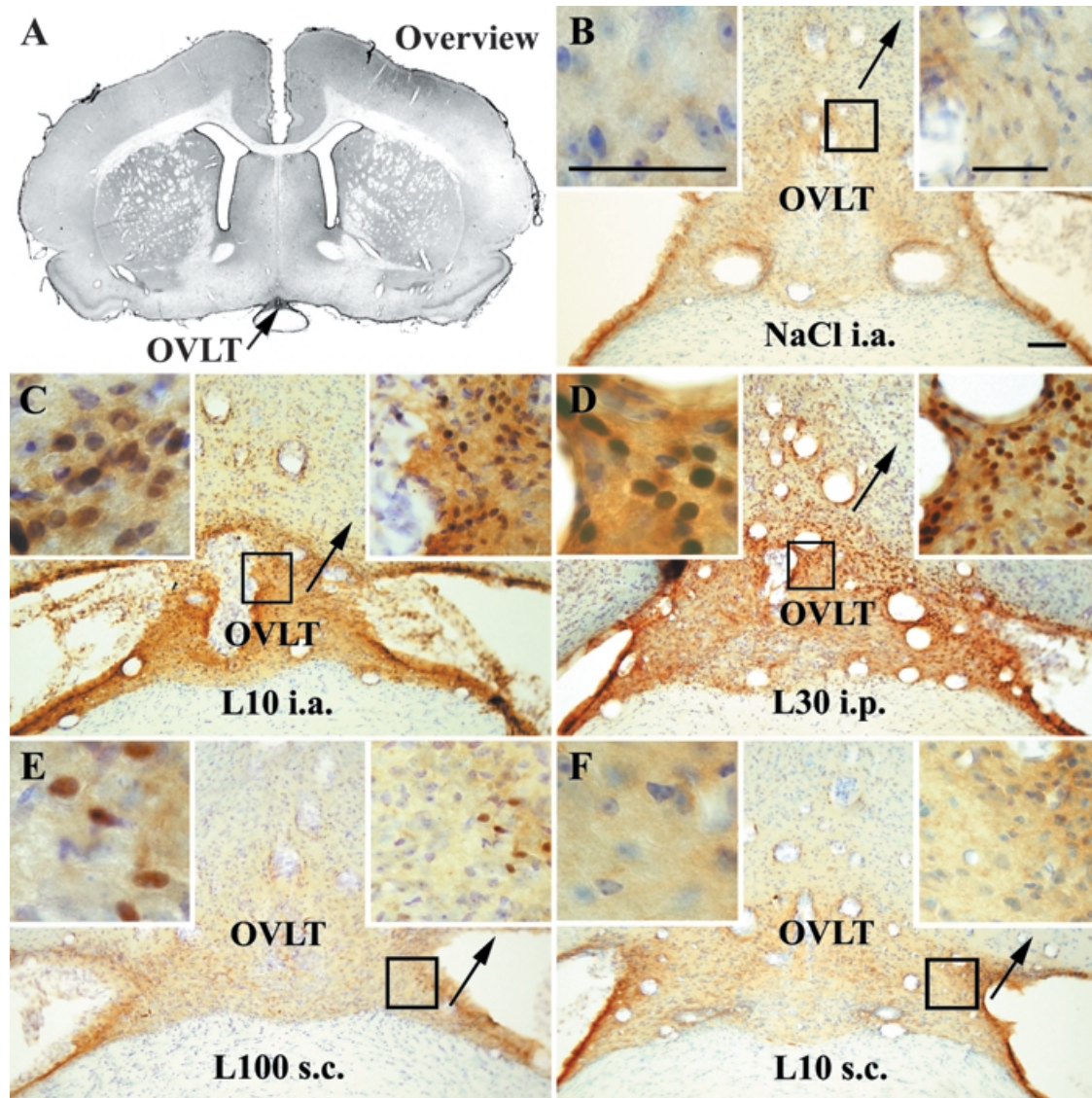

Figure 4. STAT3 immunoreactivity in the vascular organ of the lamina terminalis (OVLT) of guinea pigs injected systemically or locally with LPS or vehicle
Representative photomicrographs of the OVLT (arrows) are shown in an overview (*A*) during non-stimulated (*B*) and LPS-stimulated (*C*–*F*) conditions. Details as in legend to Fig. 3. Bar in *B* represents 100 μm. Bars in the insets represent 50 μm.

complete blood–brain barrier. Two prominent nuclei with such properties were identified as the ventromedial preoptic nucleus (VMPO) and the hypothalamic SON (Fig. 6). Although these structures are listed as areas distinct from each other, we observed a continuous band of nuclear STAT3 signals in animals systemically treated with LPS starting from rostral VMPO aspects to caudal parts of the SON. With regard to this band the most intense nuclear STAT3 immunoreactivity was observed in rostral components of the SON (Fig. 6*C* and *D*).

The mean number of nuclear STAT3 signals detected in brain sections from sensory CVOs and from the SON were counted and quantitatively evaluated (Fig. 7).

Irrespective of the route of LPS administration, the highest number of STAT3 signals always occurred in the AP. Mean numbers of about 450 STAT3-positive cell nuclei were counted in AP sections from guinea pigs treated I.A. or I.P. with LPS. This number decreased to 97 STAT3-immunoreactive nuclei in AP sections of animals injected s.c. with $100 \mu g \, kg^{-1}$ LPS. In guinea pigs treated s.c. with

$10 \mu g \, kg^{-1}$ LPS a significantly lower mean number of just three STAT3-positive cell nuclei was counted in the AP sections. Evaluation of nuclear STAT3 signals in the OVLT, the SFO, or in the SON lead to similar results; however, the absolute numbers of STAT3-positive cell nuclei per section were lower in these structures when compared to the AP. In all of these three structures the mean numbers of STAT3-positive cell nuclei were significantly higher in the groups treated I.A. or I.P. with LPS when compared to both groups that were injected s.c. with the pyrogen. In summary, the degree of LPS-induced nuclear translocation of STAT3 within sensory CVOs of the guinea pig brain depended on the route of LPS administration and corresponded to the levels of IL-6 in plasma. Remarkably, it seemed that the rather moderate rise in circulating IL-6, which is measurable in response to s.c. injections of $100 \mu g \, kg^{-1}$ LPS (in part also to s.c. injections of $10 \mu g \, kg^{-1}$), is detected by the CNS via sensory CVOs and some other brain structures in guinea pigs.
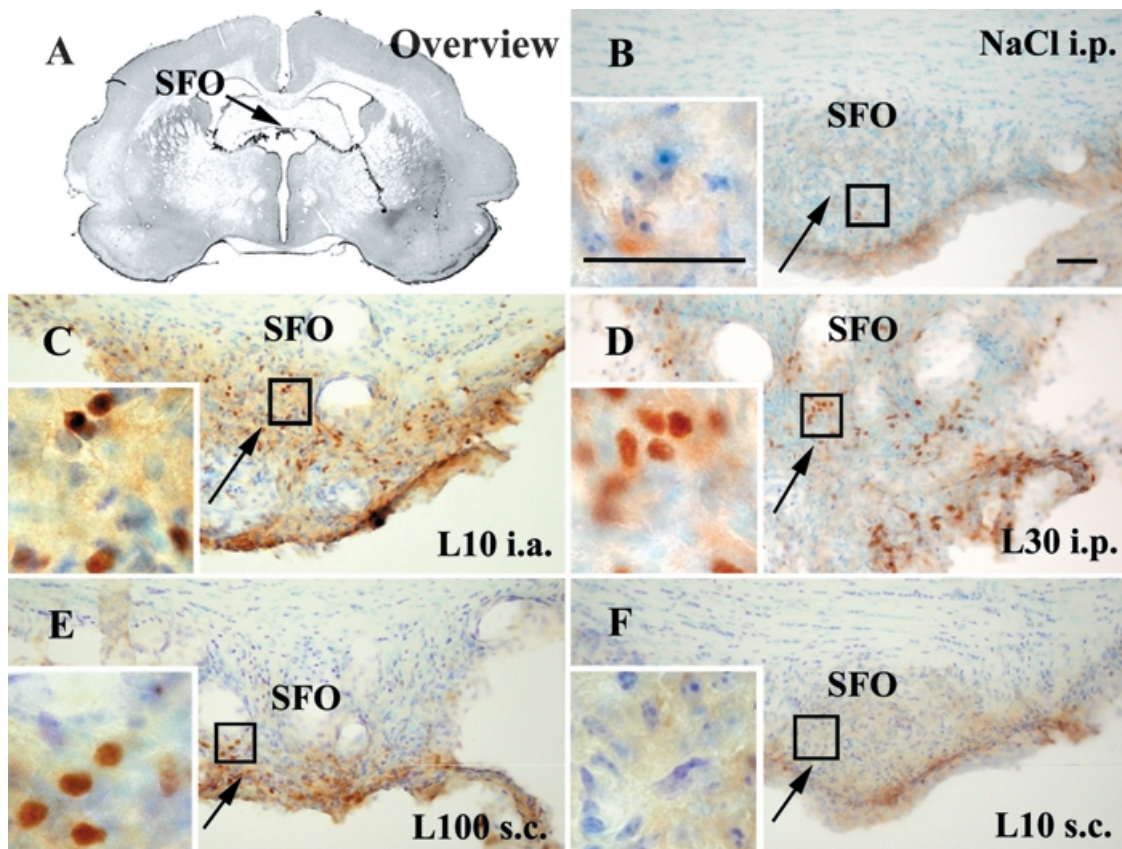

Figure 5. STAT3 immunoreactivity in the subfornical organ (SFO) of guinea pigs injected systemically or locally with LPS or vehicle
Representative photomicrographs of the medial SFO (arrows) are shown in an overview (*A*), during non-stimulated (*B*) and LPS-stimulated (*C–F*) conditions. Details as in legend to Fig. 3. Bars in *B* and the inset represent 50 μm.

Discussion

The OVLT was the first of the sensory CVOs suggested to act as a target structure within the brain for a putative 'endogenous pyrogen'. This proposal was based on the observation that electrolytic ablation of the OVLT, or disruption of neuronal connections from the OVLT to the hypothalamus, inhibit fever in response to systemic injections of pyrogens (Blatteis *et al.* 1983, 1987; Hashimoto *et al.* 1994). Later on other lesion studies also provided evidence for a role of the SFO (Takahashi *et al.* 1997), or the AP (Lee *et al.* 1998) in immune-to-brain signalling. One disadvantage of such lesion studies is that ablation of a given brain area clearly impairs all physiological functions of this structure. It has thus been argued that lesions of the lamina terminalis, which contains SFO and OVLT, might cause depression of fever by undesired side-effects such as adipsia, considerable loss of body mass, and hyperthermia (Romanovsky *et al.* 2003). However, results obtained from lesion experiments (i.e. the effects of
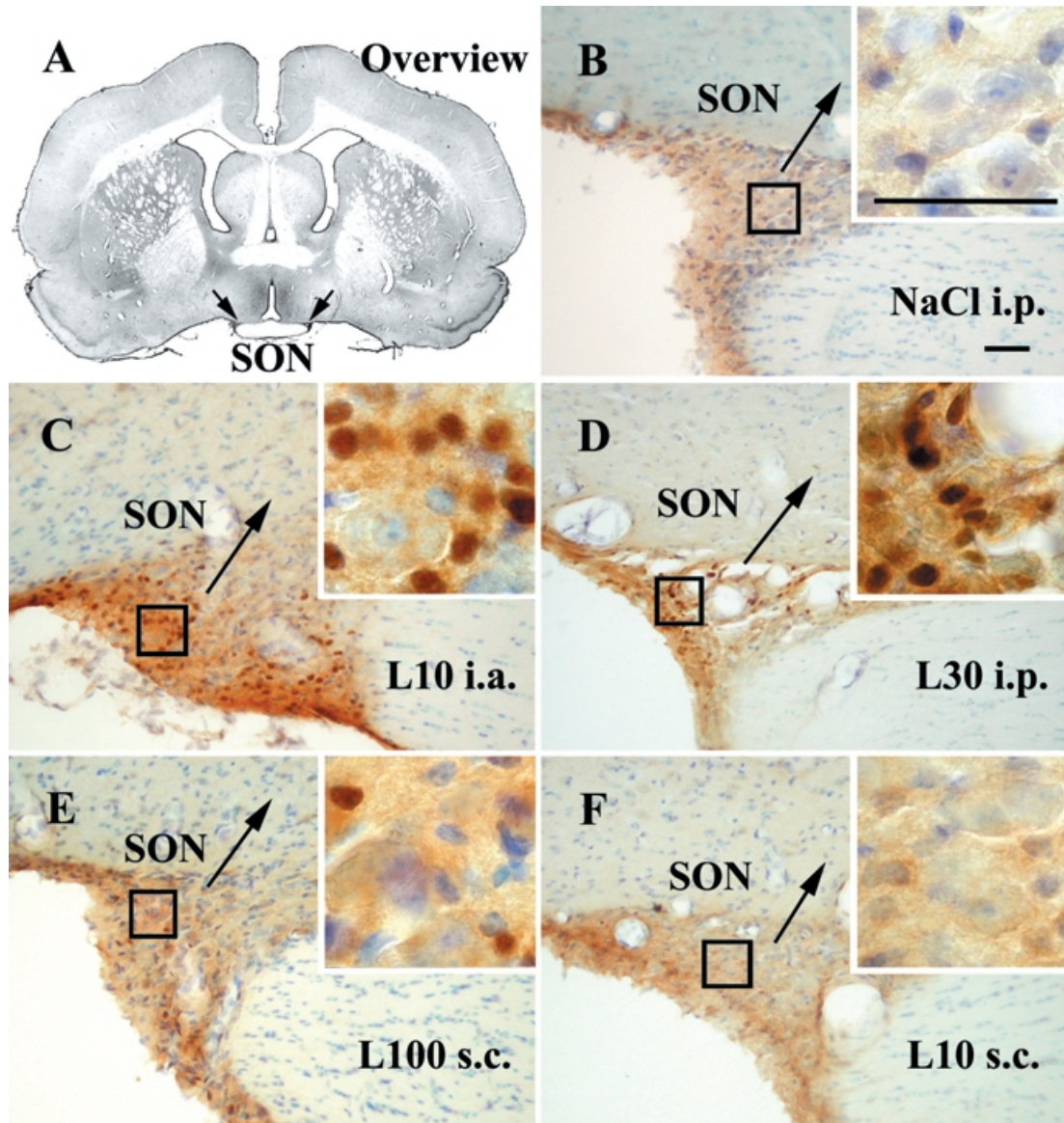

Figure 6. STAT3 immunoreactivity in the hypothalamic supraoptic nucleus (SON) of guinea pigs injected systemically or locally with LPS or vehicle
Representative photomicrographs of the rostral SON (arrows) are shown in an overview (*A*), during non-stimulated (*B*) and LPS-stimulated (*C–F*) conditions. Details as in legend to Fig. 3. Bars in *B* and the inset represent 50 μm.

destruction of single CVOs on fever) have been supported by other experimental approaches and techniques. By means of extracellular recording of neuronal activity it was shown that the discharge rate of OVLT neurones is altered by exposure to cytokines or prostaglandin E_2 in a direction that is compatible with the generation of fever (Shibata & Blatteis, 1991; Matsuda *et al.* 1992). Recently, an exciting patch clamp study of isolated SFO neurones has been published (Desson & Ferguson, 2003). In this study, physiological concentrations of IL-1β induced a transient depolarization and an increase in firing frequency of an identified population of SFO neurones. This observation was interpreted as a putative initial step for the induction of fever in response to an immune challenge. Additional studies are required to characterize possible actions of IL-6 on electrical properties of neurones located within sensory CVOs, since this cytokine (as opposed to IL-1β) is constantly elevated in the circulation during the time course of fever.

Alternatively, or additionally to changes in electrical activity of neurones, cytokines such as IL-6 might cause genomic activation of cells within sensory CVOs. Indeed, nuclear translocation of STAT3 was detected in cells of sensory CVOs after systemic injection of LPS or IL-6 in rats (Gautron *et al.* 2002; Harré *et al.* 2002). Studying STAT3 activation in the brain following administration of LPS proved thus to be an excellent tool with which to identify target cells of cytokines. In previous studies (Harré *et al.* 2002, 2003) we observed a characteristic spatial and time-

dependent pattern of specific nuclear STAT3 translocation in the rat brain in response to I.P. injections of LPS or rat recombinant IL-6. Under these experimental conditions nuclear STAT3 translocation in rats was almost exclusively observed within the OVLT and the SFO. The activation of cells within both of these CVOs occurred 120 min after administration of LPS, or 60 min after administration of IL-6. This temporal pattern of nuclear STAT3 translocation nicely corresponded to the LPS- and IL-6-induced levels of bioactive IL-6 in plasma. Fever and rise in circulating IL-6 both seem to be induced faster in guinea pigs than in rats (Jansky *et al.* 1995; Harré *et al.* 2002). In pilot experiments we detected the first LPS-induced nuclear STAT3 signals 60 min after administration of LPS. Within the following 30 min the number of nuclear STAT3 signals drastically increased to its peak. Two hours after LPS treatment nuclear LPS-induced nuclear STAT3 activation was still high, but less pronounced when compared to the 90 min time point. We therefore evaluated LPS-induced STAT3 activation in the guinea pig brain 90 min after injection of LPS or vehicle via different routes.

Cytokines are the putative endogenous mediators of LPS-induced nuclear STAT3 translocation, but IL-6 is clearly not the exclusive cytokine which is capable to induce STAT3 activation. Other cytokines such as IL-11, CNTF, LIF, or leptin are also signalling through the gp130 receptor subunit and are potentially able to induce nuclear STAT3 translocation (Taga & Kishimoto, 1997; Takeda & Akira, 2000; Hübschle *et al.* 2001). Therefore, one might argue
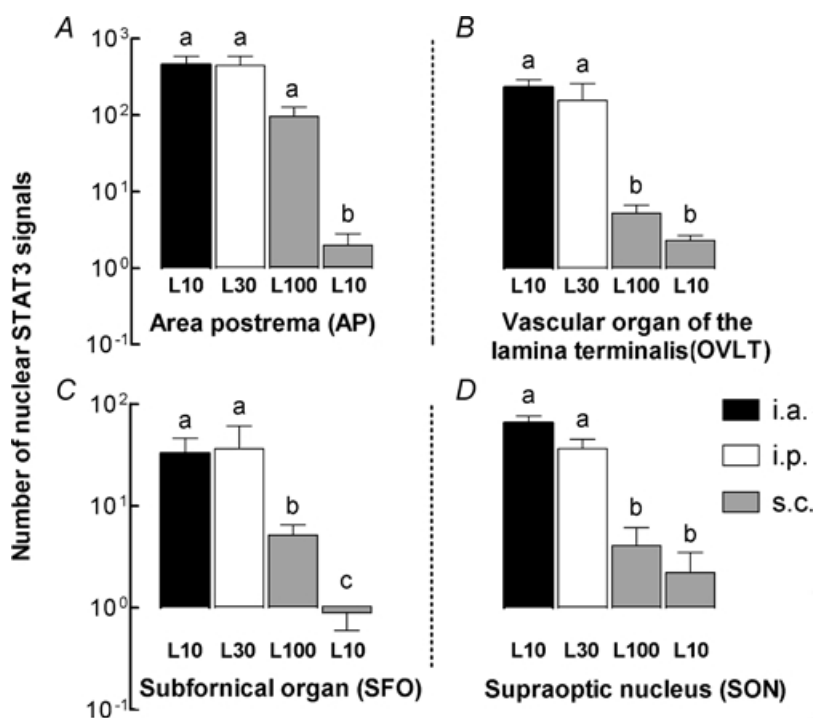

Figure 7. Number of nuclear STAT3 signals in sensory circumventricular organs (CVOs) of guinea pigs injected I.A., I.P. or S.C. with LPS or vehicle
Quantitative evaluation of the numbers of STAT3-immunoreactive cell nuclei in the AP (*A*), the OVLT (*B*), the SFO (*C*), or the SON (*D*) 90 min after I.A. injection of 10 μg kg^{-1} LPS (L10, black columns), I.P. injection of 30 μg kg^{-1} LPS (L30, open columns), S.C. injection of 100 μg kg^{-1} LPS (L100, left grey columns), or S.C. injection of 10 μg kg^{-1} LPS (L10, right grey columns). Note that within the respective control situation no nuclear signals were detected in these brain structures. Any columns with the same letter are not significantly different from each other, while any columns with different letters are significantly different ($P < 0.05$). All columns are means $\pm$ S.E.M.

that LPS is also an inducer of leptin (Fink *et al.* 1998; Francis *et al.* 1999) and that leptin thus might contribute to the observed nuclear STAT3 translocation. However, the spatial pattern of leptin-induced STAT3 activation in the brain is distinct from that induced by IL-6, irrespective of whether both cytokines were injected centrally (Hübschle *et al.* 2001) or peripherally (Harré *et al.* 2002; Hosoi *et al.* 2002). Namely in the sensory CVOs, which were of special interest for our study, no leptin-induced nuclear STAT3 translocation seems to take place (Hübschle *et al.* 2001; Hosoi *et al.* 2002).

For the following reasons we believe that most of the nuclear STAT3 signals which we observed in the guinea pig brain in response to LPS were mediated by IL-6. Pronounced circulating levels of IL-6 are induced by LPS and the strength of nuclear STAT3 translocation in sensory CVOs corresponds nicely to the concentrations of bioactive IL-6 in plasma (compare Figs 2 and 6). The IL-6 receptor and the gp130 subunit, both necessary for IL-6 signal transduction, are expressed in OVLT, SFO, AP and other brain areas even under basal conditions (Vallières & Rivest, 1997) in which we observed LPS-induced STAT3 activation. Injection of LPS even up-regulates the expression of IL-6 receptor and gp130 mRNA within the sensory CVOs and thus seems to prime these brain structures for a more powerful interaction with circulating IL-6. It should, however, be noted that IL-6 receptors, as well as gp130 subunits, are also expressed along the brain microvasculature of LPS-treated animals and that IL-6 is therefore capable of targeting the endothelium of brain capillaries (Vallières & Rivest, 1997). In addition, it might be possible that LPS stimulates the expression and release of soluble IL-6 receptors which might stimulate cells expressing gp130 in concert with IL-6.

Investigation of the transcriptional activation of the suppressor of cytokine signalling-3 (SOCS3) in the brain during systemic inflammation proved to be an alternative approach to the study of IL-6-induced brain activation (Lebel *et al.* 2000). Expression of the SOCS3 gene in a given target cell is STAT3 dependent. The product of the SOCS3 gene, in turn, inhibits STAT3 phosphorylation and thereby exerts a negative autoregulatory feedback on its own gene expression. A robust induction of the gene encoding SOCS3 is observed in rats and mice 3 h after I.P. treatment with LPS in brain vasculature and in sensory CVOs. This response is missing in IL-6-deficient mice and seems thus to be IL-6 mediated (Lebel *et al.* 2000). The time courses of nuclear STAT3 activation at the protein level in our study (peak: 90 min after LPS treatment) and of SOCS3 expression at the mRNA level in the study published by

Lebel *et al.* (2000) is compatible with the view that SOCS3 acts downstream to STAT3. The fact that nuclear STAT3 activation is toned down after its peak in spite of a further increase of circulating IL-6 (Roth *et al.* 1993) indicates that the observed nuclear STAT3 activation is depressed by SOCS3.

Interestingly, systemic treatment with LPS induced nuclear STAT3 activation in some brain areas which are regarded as structures with a complete blood–brain barrier, namely the VMPO and the SON. We observed a continuous band of nuclear STAT3 signals starting from the rostral aspects of VMPO and ending in caudal parts of the SON. The functional relevance of this observation is not clear at present. However, it should be noted that the rat VMPO has been suggested as a brain structure which represents a pyrogenic zone (Scammell *et al.* 1996). It will thus be worthwhile to investigate whether the observed genomic activation of cells in this area by circulating IL-6 can be identified as a mechanism with functional relevance for the febrile response in guinea pigs. In this context it should be noted that the observed correlation between IL-6-mediated nuclear STAT3 activation and fever does not necessarily show causation. Even if the activation of some genes in cells of sensory CVOs by circulating IL-6 are implicated in fever, it is rather unlikely that the IL-6-mediated genomic activation of brain cells is involved in the induction or in the manifestation of the first fever phase. Due to the data shown in Fig. 1 the onset of fever clearly precedes the appearance of nuclear STAT3 signals in the brain. It might, however, still be possible that genes which are activated by STAT3 participate in the maintenance of fever, namely during the second phase of the febrile response.

Corresponding to the high levels of IL-6 in plasma, administration of LPS via systemic routes induced a pronounced STAT3 activation in the guinea pig brain. Interestingly, injection of 100 μg kg^{-1} LPS s.c., the same dose which was used in the rat by Cartmell *et al.* (2000) for administration into a subcutaneous air pouch, also caused a moderate (OVLT and SFO) to high (AP) nuclear STAT3 translocation in sensory CVOs. This observation clearly supports the hypothesis suggested by Cartmell *et al.* (2000) that IL-6 which enters the circulation from a local subcutaneous site of inflammation might activate CNS mechanisms. At present we are unable to decide whether the genes which are activated by nuclear STAT3 translocation in the brain are really involved in the manifestation of fever. However, our findings indicate that the comparatively moderate amounts of IL-6 which appear in plasma after injection of 100 μg kg^{-1} LPS into the subcutaneous chamber gain entry to the brain at the

level of the sensory CVOs, namely the AP, and cause a direct genomic activation of brain cells. A putative role for circulating IL-6 as an afferent signal for the maintenance of fever (Cartmell *et al.* 2000) and HPA axis activation during localized inflammation (Turnbull *et al.* 2003) is thus supported by our study.

In response to the injection of 10 μg kg^{-1} LPS into the subcutaneous chamber we observed fever, but the small rise in circulating IL-6 hardly caused STAT3 activation in the brain. Just a few cells responded with nuclear STAT3 translocation to this stimulus. In a previous study (Ross *et al.* 2000) we showed that, to a certain extent, the fever that is induced by injecting 10 μg kg^{-1} LPS into the subcutaneous chamber can be blocked by coadministration of a local anaesthetic into the chamber. This finding supports the view that, in addition to humoral factors such as IL-6, afferent nerves might participate in the generation of fever in this experimental model. In the case of the high dose of LPS (100 μg kg^{-1} s.c.) the humoral component might override the neuronal component of the signals for fever induction and therefore treatment with the local anaesthetic could have been ineffective in this case due to the spillover of sufficient amounts of endogenous mediators (i.e. IL-6) into the systemic circulation (Ross *et al.* 2000). A role for afferent nerves in immune-to-brain signalling during inflammation has been discussed and explored experimentally during the past 10 years (Watkins *et al.* 1995; Blatteis & Sehic, 1997; Konsman *et al.* 2000). Further support for an activation of sickness responses by a neural pathway derives from a recent study in which subcutaneous injections of *Escherichia coli* caused fever, decrease in locomotor activity, and corticosterone elevation several hours before cytokines or endotoxin were detected in the plasma (Campisi *et al.* 2003). Thus it seems to be important to elucidate all pathways which may participate in immune-to-brain communication during infection or inflammation.

Perspectives for future studies

In this study we have not yet identified the cell type that responded with a nuclear STAT3 translocation due to inflammatory stimulation. Such data, however, would be of great importance and would improve our knowledge about how LPS-induced STAT3 signalling in the brain might contribute to the manifestation of brain-controlled illness responses. It has been suggested that various brain cells respond with nuclear STAT3 translocation or STAT3 phosphorylation to different *in vivo* challenges. Amongst those cells are astrocytes (Justicia *et al.* 2000; Gautron *et al.* 2002; Harré *et al.* 2003), endothelial cells (Suzuki *et al.*

2001; Gautron *et al.* 2002), ependymal cells (Hübschle *et al.* 2001; Lambert *et al.* 2001; Gautron *et al.* 2002, 2003), meningeal cells (Hübschle *et al.* 2001; Gautron *et al.* 2002; Harré *et al.* 2002), microglia (Justicia *et al.* 2000), neurones (Justicia *et al.* 2000; Hübschle *et al.* 2001; Lambert *et al.* 2001; Suzuki *et al.* 2001; Gautron *et al.* 2002; Hosoi *et al.* 2002), pinealocytes (Takamiya *et al.* 2002), pituitary endocrine cells (Gautron *et al.* 2003) and tanycytes (Lambert *et al.* 2001). However, a direct proof for the respective phenotype of STAT3-responsive brain cells was only given in few cases. Such colocalization experiments revealed that responding cell types are astrocytes, corticotropes of the anterior pituitary, microglia and neurones (Justicia *et al.* 2000; Gautron *et al.* 2002, 2003; Harré *et al.* 2003). Our own preliminary data from colocalization experiments in the guinea pig brain support the findings on astrocytes and endothelial cells as responsive cell types (authors' unpublished observations). LPS-induced nuclear STAT3 signals could be colocalized with endothelial cells (von Willebrand factor) and astrocytes (glial fibrillary acidic protein) whereas, in contrast, a colocalization with a neuronal cell marker could not be established. Nuclear STAT3 signals in endothelial cells were detected throughout the entire brain. The most pronounced numbers of STAT3-responsive astrocytes were found in sensory CVOs, but with quantitative differences being observed amongst the different CVOs. A high level of colocalization of nuclear STAT3 signals with astrocytes was observed throughout the entire AP, followed by the SFO which showed a characteristic annular distribution of colocalization at its midline level. Low levels of colocalization were detected in the OVLT. At the present stage these findings should be ranked as preliminary, particularly in the light of the great variety of different STAT3-responsive brain cells described above. The interesting question regarding the phenotype of the STAT3-responsive brain cells in response to LPS treatment clearly merits further investigations.

Two other important questions arise from the outcome of this study. The first question is related to the identification of genes which are activated by STAT3 and if there might be at least one product of these activated genes that is directly linked to fever. The second question concerns an analogous problem. As already stated above, the correlation between the appearance of IL-6, STAT3 activation of brain cells and fever does not necessarily implicate causation. The use of potent inhibitors of IL-6-induced STAT3 activation might help to find an answer to this question. Recently, a fusion protein of the gp130 and IL-6 receptor ligand binding domains has been shown to

act as a potent IL-6 inhibitor by abrogating IL-6-induced STAT3 phosphorylation (Ancey *et al.* 2003). The use of such novel tools for *in vivo* studies might be the key to demonstrating causality between STAT3 activation in the brain and a possible link to the maintenance of the febrile response to LPS.

References

Aarden LA, DeGroot ER, Schaap OL & Landsdorp PM (1987). Production of hybridome growth factors by human monocytes. *Eur J Immunol* **17**, 1411–1416.

Ancey C, Küster A, Haan S, Herrmann A, Heinrich PC & Müller-Newen G (2003). A fusion protein of the gp130 and interleukin-6Rα ligand-binding domains acts as a potent interleukin-6 inhibitor. *J Biol Chem* **278**, 16968–16972.

Banks WA, Kastin AJ & Gutierrez EG (1994). Penetration of interleukin-6 across the murine blood–brain barrier. *Neurosci Lett* **179**, 53–56.

Blatteis CM, Bealer SL, Hunter WS, Llanos QJ, Ahokas RA & Mashburh TA Jr (1983). Suppression of fever after lesions of the anteroventral third ventricle in guinea pigs. *Brain Res Bull* **11**, 519–526.

Blatteis CM, Hales JRS, McKinley MJ & Fawcett AA (1987). Role of the anteroventral third ventricle region in fever in sheep. *Can J Physiol Pharmacol* **65**, 1255–1260.

Blatteis CM & Sehic E (1997). Fever: how may circulating cytokines signal the brain? *News Physiol Sci* **12**, 1–9.

Campisi J, Hansen MK, O'Connor KA, Biedenkapp JC, Watkins LR, Maier SF & Fleshner M (2003). Circulating cytokines and endotoxin are not necessary for the activation of the sickness or corticosterone response produced by peripheral *E. coli* challenge. *J Appl Physiol* **95**, 1873–1882.

Cartmell T, Luheshi GN, Hopkins SJ, Rothwell NJ & Poole S (2001). Role of endogenous interleukin-1 receptor antagonist in regulating fever induced by localised inflammation in the rat. *J Physiol* **531**, 171–180.

Cartmell T, Luheshi GN & Rothwell NJ (1999). Brain sites of action of endogenous interleukin-1 in the febrile response to localised inflammation in the rat. *J Physiol* **518**, 585–594.

Cartmell T, Poole S, Turnbull AV, Rothwell NJ & Luheshi GN (2000). Circulating interleukin-6 mediates the febrile response to localised inflammation in rats. *J Physiol* **526**, 653–661.

Chai Z, Gatti S, Toniatti C, Poli V & Bartfai T (1996). Interleukin (IL)-6 expression in the central nervous system is necessary for fever in response to lipopolysaccharide or IL-1β: a study on IL-6-deficient mice. *J Exp Med* **183**, 311–316.

Dantzer R (2001). Cytokine-induced sickness behavior: where do we stand ? *Brain Behav Immun* **15**, 7–24.

Desson SE & Ferguson AV (2003). Interleukin 1β modulates rat subfornical organ neurons as a result of activation of a non-selective cationic conductance. *J Physiol* **550**, 113–122.

Dinarello CA (1999). Cytokines as endogenous pyrogens. *J Infect Dis* **179** (Suppl. 2), S294–S304.

Fink BN, Kelley KW, Dantzer R & Johnson RW (1998). In vivo and in vitro evidence for the involvement of tumor necrosis factor-α in the induction of leptin by lipopolysaccharide. *Endocrinology* **139**, 2278–2283.

Francis J, MohanKumar PS, MohanKumar SMJ & Quadri SK (1999). Systemic administration of lipopolysaccharide increases plasma leptin levels: blockade by soluble interleukin-1 receptor. *Endocrine* **10**, 291–295.

Gautron L, Lafon P, Chaigniau M, Tramu G & Laye S (2002). Spatiotemporal analysis of signal transducer and activator of transcription 3 activation in rat brain astrocytes and pituitary following peripheral immune stimulation. *Neuroscience* **112**, 717–729.

Gautron L, Lafon P, Tramu G & Laye S (2003). In vivo activation of the interleukin-6 receptor/gp130 signaling pathway in pituitary corticotropes of lipopolysaccharide-treated rats. *Neuroendocrinology* **77**, 32–43.

Givalois L, Dornand J, Mekaouche M, Solier MD, Bristow AF, Ixart G, Siaud P, Assenmacher I & Barbanel G (1994). Temporal cascade of plasma level surges in ACTH, corticosterone, and cytokines in endotoxin challenged rats. *Am J Physiol* **267**, R164–R170.

Goldbach JM, Roth J & Zeisberger E (1997). Fever suppression by subdiaphragmatic vagotomy in guinea pigs depends on the route of pyrogen administration. *Am J Physiol* **272**, R675–R681.

Harré EM, Roth J, Gerstberger R & Hübschle T (2003). Interleukin-6 mediates lipopolysaccharide-induced nuclear STAT3 translocation in astrocytes of rat sensory circumventricular organs. *Brain Res* **980**, 151–155.

Harré EM, Roth J, Pehl U, Kueth M, Gerstberger R & Hübschle T (2002). Selected contribution: role of IL-6 in LPS-induced nuclear STAT3 translocation in sensory circumventricular organs during fever in rats. *J Appl Physiol* **92**, 2657–2666.

Hashimoto M, Ueno T & Iriki M (1994). What role does the organum vasculosum laminae terminalis play in fever in rabbits? *Pflugers Arch* **429**, 50–57.

Heinrich P, Behrmann C, Müller-Newen J, Schaper GF & Graeve L (1998). Interleukin-6-type cytokine signaling through the gp130/Jak/STAT pathway. *Biochem J* **334**, 297–314.

Holt I, Cooper RG & Hopkins SJ (1991). Relationship between local inflammation, interleukin-6 concentration and the acute phase response in arthitic patients. *Eur J Clin Invest* **21**, 479–484.

Hosoi T, Kawagishi T, Okuma Y, Tanaka J & Nomura Y (2002). Brain stem is a direct target for leptin's action in the central nervous system. *Endocrinology* **143**, 3498–3504.

Hübschle T, Thom E, Watson A, Roth J, Klaus S & Meyerhof W (2001). Leptin-induced nuclear translocation of STAT3 immunoreactivity in hypothalamic nuclei involved in body weight regulation. *J Neurosci* **21**, 2413–2424.

Jansky L, Vybiral S, Pospisilova D, Roth J, Dornand J, Zeisberger E & Kaminkova J (1995). Production of systemic and hypothalamic cytokines during the early phase of endotoxin fever. *Neuroendocrinology* **62**, 55–61.

Johnson JD, O'Connor KA, Hansen MK, Watkins LR & Maier S (2003). Effects of prior stress on LPS-induced cytokine and sickness responses. *Am J Physiol Regul Integr Comp Physiol* **284**, R422–R432.

Justicia C, Gabriel C & Planas AM (2000). Activation of the JAK/STAT pathway following transient focal cerebral ischemia: signaling through Jak1 and Stat3 in astrocytes. *Glia* **30**, 253–270.

Kluger MJ (1991). Fever: role of pyrogens and cryogens. *Physiol Rev* **71**, 93–127.

Konsman JP, Luheshi GN, Bluthe RM & Dantzer R (2000). The vagus nerve mediates behavioral depression, but not fever, in response to peripheral immune signals: a functional anatomical analysis. *Eur J Neurosci* **12**, 4434–4446.

Lambert PD, Anderson KD, Sleeman MW, Wong V, Tan J, Hijarunguru A, Corcoran TL, Murray JD, Thabet KE, Yancopoulos GD & Wiegand SJ (2001). Ciliary neurotrophic factor activates leptin-like pathways and reduces body fat, without cachexia or rebound weight gain, even in leptin-resistant obesity. *Proc Natl Acad Sci U S A* **98**, 4652–4657.

Lebel E, Vallières L & Rivest S (2000). Selective involvement of interleukin-6 in the transcriptional activation of the suppressor of cytokine signalling-3 in the brain during systemic inflammation. *Endocrinology* **141**, 3749–3763.

Lee HJ, Whiteside MB & Herkenham M (1998). Area postrema removal abolishes stimulatory effects of intravenous interleukin-1b on hypothalamic-pituitary-adrenal axis activity and c-fos mRNA in the hypothalamic paraventricular nucleus. *Brain Res Bull* **46**, 495–503.

LeMay LG, Vander AJ & Kluger MJ (1990). Role of interleukin-6 in fever in rats. *Am J Physiol* **258**, R798–R803.

Lenczowski MJP, Van Dam AM, Poole S, Larrick JW & Tilders FJH (1997). Role of circulating endotoxin and interleukin-6 in the ACTH and corticosterone response to intraperitoneal LPS. *Am J Physiol* **273**, R1870–R1877.

Matsuda T, Hori T & Nakashima T (1992). Thermal and PGE2 sensitivity of the organum vasculosum laminae terminalis region and preoptic area in rat brain slices. *J Physiol* **454**, 197–212.

Miller AJ, Hopkins SJ & Luheshi GN (1997*a*). Sites of action of IL-1 in the development of fever and cytokine responses to tissue inflammation in the rat. *Br J Pharmacol* **120**, 1274–1279.

Miller AJ, Luheshi GN, Rothwell NJ & Hopkins SJ (1997*b*). Local cytokine induction by LPS in the rat air pouch and its relationship to the febrile response. *Am J Physiol* **272**, R857–R861.

Nijsten MWN, DeGroot ER, Duis Ten HJ, Klasen HJ, Hack CE & Aarden LA (1987). Serum levels of interleukin-6 and acute phase response. *Lancet* **2**, 921.

Paxinos G & Watson C (1998). *The Rat Brain in Stereotactic Coordinates*, 4th edn. Academic Press, San Diego, USA.

Romanovsky AA, Ivanov AI, Lenczowski MJP, Kulchitsky VA, Van Dam AM, Poole S, Homer LD & Tilders FJH (2000). Lipopolysaccharide transport from the peritoneal cavity to the blood: is it controlled by the vagus nerve? *Auton Neurosci* **85**, 133–140.

Romanovsky AA, Sugimoto N, Simons CT & Hunter WS (2003). The organum vasculosum laminae terminalis in immune-to-brain febrigenic signaling: a reappraisal of lesion experiments. *Am J Physiol Regul Integr Comp Physiol* **285**, R420–R428.

Ross G, Hübschle T, Pehl U, Braun HA, Voigt K, Gerstberger R & Roth J (2003). Fever induction by localized subcutaneous inflammation in guinea pigs: the role of cytokines and prostaglandins. *J Appl Physiol* **94**, 1395–1402.

Ross G, Roth J, Störr B, Voigt K & Zeisberger E (2000). Afferent nerves are involved in the febrile response to injection of LPS into artificial subcutaneous chambers in guinea pigs. *Physiol Behav* **71**, 305–313.

Roth J, Conn CA, Kluger MJ & Zeisberger E (1993). Kinetics of systemic and intrahypothalamic IL-6 and tumor necrosis factor during endotoxin fever in guinea pigs. *Am J Physiol* **265**, R653–R658.

Roth J, McClellan JL, Kluger MJ & Zeisberger E (1994). Attenuation of fever and release of cytokines after repeated injections of lipopolysaccharide in guinea pigs. *J Physiol* **477**, 177–185.

Roth J, Martin D, Störr B & Zeisberger E (1998). Neutralization of pyrogen-induced tumour necrosis factor by its type 1 soluble receptor in guinea pigs: effects on fever and interleukin-6 release. *J Physiol* **509**, 267–275.

Scammell TE, Elmquist JK, Griffin JD & Saper CD (1996). Ventromedial preoptic prostaglandin E2 activates fever-producing autonomic pathways. *J Neurosci* **16**, 6246–6254.

Shibata M & Blatteis CM (1991). Human recombinant tumor necrosis factor and interferon affect the activity of neurons in the organum vasculosum laminae terminalis. *Brain Res* **562**, 323–326.

Strömberg H, Svensson SP & Hermanson O (2000). Distribution of the transcription factor signal transducer and activator of transcription 3 in the rat central nervous system and dorsal root ganglia. *Brain Res* **853**, 105–114.

Suzuki S, Tanaka K, Nogawa S, Dembo T, Kosakai A & Fukuuchi Y (2001). Phosphorylation of signal transducer and activator of transcription-3 (Stat3) after focal cerebral ischemia. *Exp Neurol* **170**, 63–71.

Taga T & Kishimoto T (1997). Gp130 and the interleukin-6 family of cytokines. *Annu Rev Immunol* **15**, 797–819.

Takahashi Y, Smith P, Ferguson A & Pittman QJ (1997). Circumventricular organs and fever. *Am J Physiol* **273**, R1690–R1695.

Takamiya A, Takeda M, Yoshida A & Kiyama H (2002). Inflammation induces serin protease inhibitor 3 expression in the rat pineal gland. *Neuroscience* **113**, 387–394.

Takeda K & Akira S (2000). STAT family of transcription factors in cytokine-mediated biological responses. *Cytokine Growth Factor Rev* **11**, 199–207.

Turnbull AV, Prehar S, Kennedy AR, Little RA & Hopkins SJ (2003). Interleukin-6 is an afferent signal to the hypothalamo-pituitary-adrenal axis during local inflammation in mice. *Endocrinology* **144**, 1894–1906.

Vallières L & Rivest S (1997). Regulation of the genes encoding interleukin-6, its receptor, and gp130 in the rat brain in response to immune activator lipopolysaccharide and the proinflammatory cytokine interleukin-1β. *J Neurochem* **69**, 1668–1683.

Watkins LR, Maier SF & Goehler LE (1995). Cytokine-to-brain communication: a review and analysis of alternative mechanisms. *Life Sci* **57**, 1011–1026.

Acknowledgements

Supplementary material

The online version of this paper can be found at:
DOI: 10.1113/jphysiol.2003.058834
http://www.jp.physoc.org/cgi/content/full/jphysiol.2004.058834/DC1
and contains supplementary material consisting of a figure entitled: Preabsorption control experiments to document the specificity of STAT3 immunohistochemistry in guinea pigs.
This material can also found at:
http://www.blackwellpublishing.com/products/journals/suppmat/tjp200/tjp200sm.htm